Science of the Total Environment 511 (2015) 489–500

Contents lists available at ScienceDirect

Science of the Total Environment

journal homepage: www.elsevier.com/locate/scitotenv

# Total- and methyl-mercury concentrations and methylation rates across the freshwater to hypersaline continuum of the Great Salt Lake, Utah, USA

William P. Johnson [a,*], Neil Swanson [a], Brooks Black [a], Abigail Rudd [b], Greg Carling [c], Diego P. Fernandez [a], John Luft [d], Jim Van Leeuwen [d], Mark Marvin-DiPasquale [e]

[a] Department of Geology and Geophysics, University of Utah, Salt Lake City, UT 84112, United States
[b] Brooks-Rand LLC, 4415 6th Ave NW, Seattle, WA 98107, United States
[c] Department of Geological Sciences, Brigham Young University, Provo, UT 84602, United States
[d] State of Utah Division of Wildlife Resources, 1594 W North Temple, Suite 2110, Box 146301 Salt Lake City, UT 84114, United States
[e] United States Geological Survey, Menlo Park, CA 94025, United States

## HIGHLIGHTS

- Highest Great Salt Lake methyl mercury concentrations occur in deep brine layer.
- Deep brine layer is proximal to highest reported mercury burdens reported in birds.
- Methylation rates in the deep brine layer are lowest during mid-summer.
- Mid-summer is when mercury burdens are reported lowest in aquatic invertebrates.

## GRAPHICAL ABSTRACT

## ARTICLE INFO

*Article history:*
Received 25 August 2014
Received in revised form 27 December 2014
Accepted 27 December 2014
Available online xxxx

Editor: Mae Mae Sexauer Gustin

*Keywords:*
Aqueous geochemistry
Limnology
Toxic elements
Trace elements

## ABSTRACT

We examined mercury (Hg) speciation in water and sediment of the Great Salt Lake and surrounding wetlands, a locale spanning fresh to hypersaline and oxic to anoxic conditions, in order to test the hypothesis that spatial and temporal variations in Hg concentration and methylation rates correspond to observed spatial and temporal trends in Hg burdens previously reported in biota. Water column, sediment, and pore water concentrations of methylmercury (MeHg) and total mercury (THg), as well as related aquatic chemical parameters were examined. Inorganic Hg(II)-methylation rates were determined in selected water column and sediment subsamples spiked with inorganic divalent mercury ($^{204}$Hg(II)). Net production of Me$^{204}$Hg was expressed as apparent first-order rate constants for methylation ($k_{meth}$), which were also expanded to MeHg production potential (MPP) rates via combination with tin reducible 'reactive' Hg(II) ($Hg(II)_R$) as a proxy for bioavailable Hg(II). Notable findings include: 1) elevated Hg concentrations previously reported in birds and brine flies were spatially proximal to the measured highest MeHg concentrations, the latter occurring in the anoxic deep brine layer (DBL) of the Great Salt Lake; 2) timing of reduced Hg(II)-methylation rates in the DBL (according to both $k_{meth}$ and MPP) coincides with

* Corresponding author.
*E-mail address:* william.johnson@utah.edu (W.P. Johnson).

http://dx.doi.org/10.1016/j.scitotenv.2014.12.092

reduced Hg burdens among aquatic invertebrates (brine shrimp and brine flies) that act as potential vectors of Hg propagation to the terrestrial ecosystem; 3) values of $k_{meth}$ were found to fall within the range reported by other studies; and 4) MPP rates were on the lower end of the range reported in methodologically comparable studies, suggesting the possibility that elevated MeHg in the anoxic deep brine layer results from its accumulation and persistence in this quasi-isolated environment, due to the absence of light (restricting abiotic photo demethylation) and/or minimal microbiological demethylation.



## 1. Introduction

### 1.1. Reported mercury burdens in higher biota

The Great Salt Lake (GSL), located in northwestern Utah, USA (Fig. 1), is the largest terminal lake in the Western Hemisphere, and an important ecosystem for millions of migratory birds. It is recognized as a site of hemispheric importance by the Western Hemisphere Shorebird Reserve Network, with over 1.4 million shorebirds using the GSL and surrounding wetlands for breeding and staging areas (Aldrich and Paul, 2002), and over seven million waterbirds utilizing the GSL and its associated wetlands during some portion of their biannual migration (Cline et al., 2011). Human consumption advisories are in place for three GSL duck species among seven examined (Scholl and Ball, 2005, 2006), based on breast muscle tissue mercury (Hg) concentrations exceeding the EPA screening value of 0.3 mg-kg$^{-1}$ ww (USEPA, 2000). Several important spatial and temporal trends are suggested by existing studies of elevated mercury concentrations among avian species at GSL:

1) Hg concentrations in multiple migratory species increase during the fall season; e.g., eared grebes, which consume primarily brine shrimp from GSL during the fall molting period showed factor of three increased median liver Hg concentrations during the 3–5 month fall molting period (Naftz et al., 2008a), and eared grebe blood Hg concentrations that spent the fall of 2006 on GSL were shown to be higher in November than September, and were greater for adults relative to juveniles (Vest et al., 2008; Conover and Vest, 2009a). A trend towards elevated levels of liver Hg concentrations in autumn-collected waterfowl at Ogden Bay wetlands was observed in 2008 (Cline et al., 2011); however, it was not determined whether these birds arrived on the lake with that exposure or if they were exposed to Hg via the GSL open-water food chain, or in the wetlands.
2) Blood Hg concentrations in eared grebes that spent the fall of 2006 on GSL were higher at Stansbury Island on the west side of Gilbert Bay (Fig. 1) (10.1 ± 2.6, n = 30) relative to Antelope Island on the east side of Gilbert Bay (4.3 ± 0.5 mg kg$^{-1}$, n = 30) (Conover and Vest, 2009);
3) Elevated Hg concentrations vary inter-annually among avian species, as indicated by results collected in 2008 (Cline et al., 2011), where the mean Hg concentrations in adult breast muscle did not exceed the EPA screening level of 0.3 mg kg$^{-1}$ ww, except for adults of one species only during the spring season only. This contrasts with the preceding studies showing highly elevated Hg burdens, and suggests inter-annual variation over several year periods (2005–2008).

### 1.2. Reported Hg concentrations in the aquatic system

At approximately the same time that high Hg concentrations were recognized in some waterfowl on the GSL in 2007, exceptionally high MeHg concentrations were found in the anoxic deep brine layer (DBL) of the GSL (Naftz et al., 2008), ranging beyond 30 ng-L$^{-1}$. The DBL occupies the deepest portions of the GSL at depths (during the study) from approximately 6.5 to 9 m below the surface (Baskin, 2005; Diaz et al., 2009). The DBL arises from a strong salinity contrast between the north and south arms of the GSL, which are separated by a railroad causeway. Higher salinity water flows from the north to the south arm through breaches in the causeway (and the permeable fill material), and pools in the south arm of the lake. This high salinity bottom water is not subject to annual turnover because of the strong and persistent density differences between the upper and lower water bodies (Naftz et al., 2008; Gwynn, 2002; Loving et al., 2002). Since MeHg is the bioaccumulative form of Hg (Baeyens et al., 2003; Mason et al., 2006), these high MeHg concentrations in the DBL indicate a possible connection to elevated Hg in waterfowl.

Reactive gaseous mercury (RGM) is produced within the GSL basin on the basis that a regular diel pattern in RGM concentrations was observed regardless of season and boundary layer height (Peterson and Gustin, 2008). Measured cumulative annual riverine Hg load to the GSL (~6 kg) (Naftz et al., 2009) was far less than measured cumulative annual atmospheric deposition load (~36 kg) (Peterson and Gustin, 2008). With respect to aquatic geochemical processes, the DBL has unique characteristics relative to typical surface water bodies, including: a) anoxia (Gwynn, 2002; Diaz et al., 2009b) high activity levels of sulfate reducing bacteria (Naftz et al., 2009; Ingvorsen and Brandt, 2002);and c) high organic carbon content ca. 60–90 mg-L$^{-1}$ (Diaz et al., 2009, Supporting information); all of which have been associated with MeHg production (King et al., 2000; Sunderland et al., 2006; Graham et al., 2012). The above characteristics suggest that the DBL may have uniquely high Hg(II)-methylation rates relative to other water bodies.

The eventual propagation of Hg from the DBL to shallow portions of GSL is suggested by direct measurement of at least limited mixing that occurs during wind events (Beisner et al., 2009), and by high north-to-south velocities measured in the DBL (Beisner et al., 2009) that suggest relatively rapid convection and imply eventual re-entrainment of DBL into the shallow brine layer at the south end of the GSL. Water column depths in the overall GSL system range from ~9 m in the main body of the GSL to approximately 1–1.5 m in the impounded wetlands and shallow portions of the freshwater-influenced bays to (Fig. 1). The impounded wetlands experience diel cycles in water column pH, dissolved oxygen (DO), and trace elements (e.g., selenium, antimony, manganese), with the greatest diel swings occurring during summer (Dicataldo et al., 2010; Carling et al., 2011). Despite diel and seasonal variations, wetland surface water, pore water, and sediment show major and trace element chemistries that occupy unique locations in non-metric multidimensional scaling (NMS) space. These locations in NMS space correspond to proximity of the wetland to, for example, metropolitan effluent and hypersaline GSL water (Carling et al., 2013). The Impounded wetlands contain freshwater, whereas pore water in the western-most Sheetflow wetlands have elevated salinity due to periodic encroachment by saline water from Farmington Bay, a freshwater-influenced bay of GSL. Pintail, an impounded pond at the north end of the system that is groundwater fed, shows elevated salinity relative to other freshwater wetlands in the system (Carling et al., 2013).

### 1.3. Reported Hg burdens in lower biota

The above-described Hg burdens in multiple avian species and exceptional MeHg concentrations in at least one aquatic settling highlight the need to understand potential pathways of Hg bioaccumulation in this hydrologic system that also has a constrained food web. Specifically, salinities >120 g L$^{-1}$ in most parts of the GSL exclude predacious fish, so

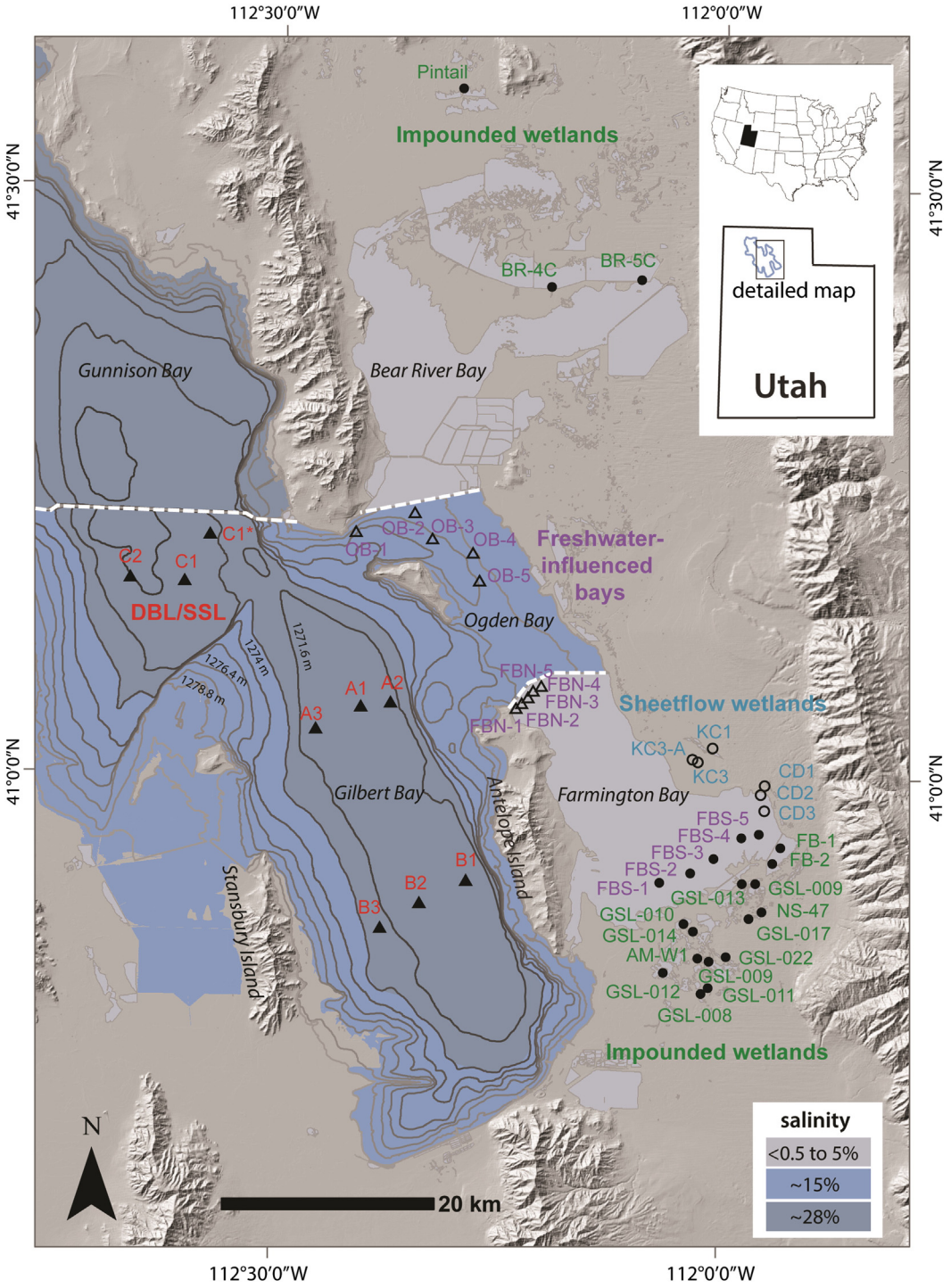


**Fig. 1.** Locations sampled in the continuum from freshwater (Impounded and Sheetflow) wetlands to Freshwater-influenced bays to hypersaline (GSL Gilbert Bay DBL and SSL). Shading represents typical salinities (% total dissolved solids) observed during the study, equal to approximately 28% (Gunnison Bay and DBL in Gilbert Bay), approximately 15% (Ogden Bay and shallow brine layer that overlies the DBL in Gilbert Bay), and ranging from 5% to <0.5% (Freshwater-influenced Bear River and Farmington Bays). Closed circles indicate Impounded wetlands, open circle — Sheetflow wetlands, closed triangles — the deep brine layer, and open triangles — Freshwater-influenced bays.

that birds constitute the sole predator of invertebrates produced in the open water system (Wurtsbaugh et al., 2011). With respect to aquatic invertebrates that potentially convey Hg from open water aquatic reservoirs to terrestrial invertebrates, the lake's pelagic zone produces abundant brine shrimp (*Artemia franciscana*), and the only other abundant macroinvertebrate is the brine fly (*Ephydra gracilis*), which feed primarily on periphyton growing on, and forming the abundant carbonaceous biostromes (stromatolites) that cover 260 km$^2$ of the lake's shallow littoral zone, with a biomass that rivals that of *Artemia* in the water column (Wurtsbaugh et al., 2011). Two intriguing trends are suggested by the limited measured Hg concentrations in aquatic invertebrates:

1) Brine fly Hg concentrations were significantly higher at Stansbury Island (west side of Gilbert Bay) relative to samples obtained from the eastern side of the south arm of GSL (Wurtsbaugh et al., 2011), similar to the spatial relationship previously observed for Hg in eared grebes (Conover and Vest, 2009);

2) Aquatic invertebrates showed reduced Hg burdens in mid-summer (July) relative to other sampling periods. This temporal trend was observed for adult brine shrimp (Peterson and Gustin, 2008; Van Leeuwen et al., 2011), and brine flies (Wurtsbaugh et al., 2011). More recently, monthly THg concentrations in brine flies measured at two locations on Antelope Island in 2012 showed lowest values in June–July (~100 to 200 mg $kg^{-1}$) versus highest values in March–April (~200 to 500 mg $kg^{-1}$) (Frank Black, personal communication).

### 1.4. Objectives of the study

The above results for Hg concentrations in higher and lower biota suggest some general spatial and temporal trends, specifically: 1) greater elevated Hg burdens in avian species on the west side relative to the east side of Gilbert Bay; 2) minimum Hg burdens in aquatic invertebrates (adult brine shrimp and brine flies) during mid-summer (July). On the basis of these spatial and temporal differences in Hg burden among lower and higher trophic levels, reported in multiple studies summarized above, we posit that a survey of THg and MeHg concentrations across the freshwater to hypersaline continuum of the GSL will show correspondence; that is, proximity of locations of highest MeHg concentrations in water and sediment to locations of highest Hg burdens reported in biota. Furthermore, assuming that the DBL is the primary reservoir from which MeHg propagates into the ecosystem, we expect that Hg(II)-methylation rates and perhaps MeHg concentrations in the DBL will show correspondence with temporal variation in burdens among the ecosystem.

## 2. Methods

### 2.1. Locations, sampling, and field methods

Three aquatic settings in the system were examined for THg and MeHg concentrations: south arm (main body) of the GSL (6 sites), freshwater influenced bays (Ogden and Farmington Bays, 15 sites), impounded freshwater wetlands (16 sites), and sheet flow wetlands (5 sites) (Fig. 1). At impounded freshwater wetlands, samples were collected near the pond outfall to integrate concentrations across the water body.

Three types of media were collected from these locations: water column, sediment, and sediment pore water, with the exception that water column samples were not collected in the sheet flow wetlands (negligible water column depth) and pore water was not collected in the freshwater-influenced bays. The target water column in the south arm of GSL was the DBL, a hypersaline lens with a thickness of ~2.0 m (Diaz et al., 2009). The target sediment in the GSL was the fine, unconsolidated, organic rich sediment slurry underlying the DBL. Water column samples from the DBL and freshwater-influenced bay were unfiltered, except where specifically stated otherwise. All impounded wetland water column and pore water samples were filtered (0.45 μm PES membrane).

Samples were collected during the period from May 2009 to December 2012. In the south arm of the GSL, three transects were sampled in August 2011 (3 sites each), and April and July 2012 (2 sites each). In freshwater-influenced Ogden and Farmington Bays (OB and FB, respectively), five-site transects were sampled in late July and October 2009 at FB and in August 2010 at OB. In the Freshwater impounded wetlands, 16 locations were sampled throughout summer 2012 and 5 corresponding locations throughout summer 2010–2011, with varying frequency of 2-to-4 times each summer. In the Sheet flow wetlands, 5 locations were sampled during June and July 2011.

Methods used for collecting samples from the above three media are described in detail in the Supporting information. Pore water sampling methods were adapted from Chin et al. (1998). Field measurements included dissolved oxygen (DO), temperature (T), conductivity, and pH, all measured in the water column using a field probe (YSI Quatro Professional Series). Sulfide was measured on filtered water column and pore water samples immediately after collection (V-2000 Multi-analyte LED Photometer and Vacu-vials®, CHEMetrics).

### 2.2. Purification and concentration analyses

Sample preparation for analyses depended on the sample medium and target analyte. Extraction for analysis of sediment constituents was performed according to USEPA Method 1631 (2001b) for THg, Bloom et al. (1997) for MeHg, Marvin-DiPasquale and Cox (2007) for reactive inorganic Hg, ($Hg(II)_R$), and Carling et al. (2011) for trace elements. Analysis of aqueous samples (including post-extraction) was performed according to USEPA Method 1631 (2002) (THg) and USEPA Method 1630 (2001a) (MeHg), and Marvin-DiPasquale and Cox (2007) ($Hg(II)_R$). For MeHg concentrations related to determining methylation and demethylation, isotope dilution (ID) correction was used (described below). Inorganic ($^{204}$Hg(II), Oak Ridge National Laboratory) and methyl ($Me^{201}$Hg, Applied Isotope Technologies) Hg isotopic tracers were mixed with DBL, SSL, and impounded wetland samples and, after purification and trapping (as further described in Supporting information), detected via inductively coupled plasma mass-spectrometry (ICP-MS) (Agilent 7500ce). Hg released from thermal desorption (gold or carbon traps) was transported into the ICP-MS under an argon flow using a custom made PTFE interface connected directly to the torch injector. All measurements (except $Hg(II)_R$) were performed at the University of Utah. $Hg(II)_R$, an estimation of bioavailable Hg (II) using $SnCl_2$ reduction (Marvin-DiPasquale and Cox, 2007) followed by CVAFS, was performed at the USGS (Menlo Park, CA). These methods and associated quality control monitoring are described in detail in the Supporting information. Using isotopically-enriched Hg(II) and MeHg, methylation and demethylation was characterized across this range of settings, including the near-surface sediment usually considered to be the primary zone of net MeHg production (Choi and Bartha, 1994; Gilmour et al., 1998; Marvin-DiPasquale et al., 2003; Marvin-DiPasquale and Agee, 2003).

### 2.3. Spiking and equilibration

Methylation and demethylation rates were determined in select samples spiked with $^{204}$Hg(II) and $Me^{201}$Hg, respectively. These samples were prepared under argon in a glove box (Vacuum Glovebox VGB, MTI Corporation), within 12 h of sample collection. Isotope tracer concentrations were targeted to match ambient THg and MeHg concentrations (total of all isotopes). However, not all ambient THg and MeHg concentrations were known a priori, in which case estimates were made based on previously existing data. $^{204}$Hg(II) and $Me^{201}$Hg tracer amendment concentrations were within a factor of three of ambient concentrations for 74% and 65% of samples, respectively. These amendments were within a factor of 10 of ambient concentrations for 97% ($^{204}$Hg(II)) and 85% ($Me^{201}$Hg) of samples. A complete table of isotope tracer amendment concentrations (represented as % ambient concentrations) is provided in the Supporting information. $^{204}$Hg(II) and $Me^{201}$Hg amendments were pipetted to each sample aliquot (200 g water column, 50 g sediment) and homogenized by subsequent stirring.

Following isotope addition, samples were subdivided to allow multiple incubation times in parallel subsamples. Subsamples were placed into crimp-top serum bottles with chlorobutyl-isoprene blend septa (50 mL bottles for water column samples, and 10 mL bottles for sediment slurries from wetlands and SSL below DBL). Subsamples were replicated to allow analysis of pre- and post-amended samples, and to allow correction for extraction inefficiencies via isotope dilution (described below). Subsample incubations were performed at room temperature (19–21 °C) on a shaker table (130 rpm). Incubations were arrested after 2, 4, and 10 h (GSL), and 12, 24, 48, and 72 h (freshwater influenced bays and impounded wetlands) via the addition of

trace metal grade HCl (1% v-v$^{-1}$) and refrigeration (water column samples), or via flash freezing (ethanol bath in −20 °C freezer) (sediment and SSL samples).

For GSL methylation/demethylation subsamples, an isotope dilution (ID) spike, $Me^{200}Hg$ was added prior to distillation (water column samples) or extraction (SSL samples) via glass syringe through chlorobutyl-isoprene blend septa. ID spike concentrations were matched to ambient when known, and otherwise were based on the most recent existing data. ID spike concentrations were within a factor of 3-to-10 of ambient MeHg concentrations for 75% and 95% of samples, respectively (Supporting information Table S3). Following ID spike addition, the sample was allowed to equilibrate for 15 min before extraction. The time period following tracer isotope addition over which samples remained frozen before thawing, ID spike addition, and analysis was at most one month for water samples and three months for sediment.

### 2.4. Kinetic analysis

Isotope dilution (ID) was used to correct for extraction inefficiencies in determining isotope concentrations, based on recovery of the ID isotope ($Me^{200}Hg$) as follows (Hintelmann and Evans, 1997).

$$C_{204}^{preID} = \frac{m_{204}^{Me200ID}\left(R_{\frac{200}{204}}^{Me200ID} - R_{\frac{200}{204}}^{postID}\right)}{sample\ mass\left(R_{\frac{200}{204}}^{postID} - R_{\frac{200}{204}}^{preID}\right)} \quad (1)$$

where, $C^{preID}{}_{204}$ is the ID-corrected concentration of $Me^{204}Hg$, $m^{Me200ID}{}_{204}$ is the mass of $Me^{204}Hg$ in the enriched Me $^{200}Hg$ ID spike, $R^{Me200ID}{}_{200/204}$ is the ratio of $Me^{200}Hg$ to $Me^{204}Hg$ in the ID spike, $R^{postID}{}_{200/204}$ is the ratio of $Me^{200}Hg$ to $Me^{204}Hg$ in the sample post ID spike addition, $R^{preID}{}_{200/204}$ is the ratio of $Me^{200}Hg$ to $Me^{204}Hg$ in the sample pre ID spike addition and *sample mass* corresponds to that which the ID spike was added.

Finite difference was used to back-out net methylation and demethylation rate constants ($k_{meth}$ and $k_{demeth}$, respectively) from either the ID-corrected concentrations (GSL samples) or isotopic ratios (GSL, freshwater-influenced bay, and wetland samples). $k_{meth}$ and $k_{demeth}$ were determined from ID-corrected concentrations according to the equations below (Marvin-DiPasquale et al., 2008):

$$k_{meth} = \ln[1-f_m]/t \quad (2)$$

$$k_{demeth} = ln[1-f_d]/t \quad (3)$$

where $f_m$ is the fraction of [$^{204}Hg(II)$] converted to [$Me^{204}Hg$], $f_d$ is the fraction of [$Me^{201}Hg$] converted to [$I^{201}Hg$] (brackets here refer to concentrations), and $t$ is the time of incubation. $k_{meth}$ was also determined from isotopic ratios by numerical approximation of the methylation/demethylation process according to the equation below:

$$\left[Me^iHg\right]_t = \left[Me^iHg\right]_{t-1} + k_{meth}\left[{}^iHg(II)\right]_{t-1}\Delta t - k_{demeth}\left[Me^iHg\right]_{t-1}\Delta t \quad (4)$$

where the time series was simulated for all measured MeHg isotopes ($i$ = 200, 201, 202, 204), $t$ and $t-1$ represent present and previous time steps, respectively, and $\Delta t$ is the length of the time step. Because the conditions influencing $k_{meth}$ and $k_{demeth}$ (e.g., [$SO_4^{2-}$], [$S^{2-}$]) in the serum vials likely evolved over the course of incubation, the concentrations corresponding to the first two sample times were emphasized to determine $k_{meth}$ and $k_{demeth}$. Under the reasonable assumption that rate constants were equivalent for all isotopes, Eq. ((4) provides two equations (for isotopes 204 and 201) with two unknowns ($k_{meth}$ and $k_{demeth}$).

Our methods for estimating Hg(II)-methylation rates evolved over several years. Initially, we used isotopic ratios (Eq. (4) to estimate $k_{meth}$ and $k_{demeth}$ on samples from the freshwater-influenced bays and impounded wetlands. Subsequently, we used ID correction for concentrations (Eqs. (1)–(3)) of DBL and sediment slurry samples from the south arm of GSL. For the latter set of samples, values of $k_{meth}$ and $k_{demeth}$ were obtained using both ID-corrected concentrations (Eqs. 1–3) and isotope ratios (Eq. (4). Both methods produced similar rate constants, demonstrating that a single rate constant was able to fit trends in both ID-corrected concentrations and isotope ratios effectively. These fits are shown for all sites (DBL and SSL) in the Supporting information (Figure S4). Overall, the discrepancy between ID-corrected- and isotope ratio-based $k_{meth}$ values (measured as the absolute value of the difference normalized to the ID-corrected $k_{meth}$ value) was small. The maximum and average discrepancies were 84% and 39% (SSL), and 24% and 11% (DBL). These discrepancies are small relative to the factors of 10 and 30 variation, respectively, in the SSL and DBL $k_{meth}$ values. Demethylation results were considered not representative of potential in-situ conditions due to light exposure in the laboratory, and are provided and discussed in the Supporting information.

MPP rates (units = ng-kg$^{-1}$-h$^{-1}$) were calculated as a function of $k_{meth}$ and $Hg(II)_R$ according to the equation below:

$$MPP = \left[Hg(II)_R - Hg(II)_R \cdot \exp(-k_{meth}\cdot t)\right]/t \quad (5)$$

where $t$ is time (hours), and $Hg(II)_R$ refers to SSL wet weight concentrations and DBL mass concentrations.

### 2.5. Other analyses

Analysis of carbon content in aqueous and sediment media were performed according to USEPA Method 1684 (2001c) and as described in detail in the Supporting information. Trace and major elements were measured using a quadrupole ICP-MS according to USEPA Method 200.8 (1994) and as described in the Supporting information and Carling et al. (2013). While Hg(0) was not measured in the majority of our samples, it was found to be negligible in DBL samples during measurements made to support $Hg(II)_R$ analyses.

## 3. Results and discussion

### 3.1. Water

Mean concentrations (and standard deviations for replicates) of THg, MeHg, sulfide, sulfate, DOC, and pH, in surface and pore water (from ambient non-incubated samples) among the various aquatic settings are presented in Fig. 2. Note that pH was not measured in every pore water sample due to limited sample volumes. Figures, and a spreadsheet, providing specific sample locations and corresponding data within each setting are provided in the Supporting information. Across the continuum from freshwater to hypersaline settings, the highest mean MeHg concentrations in water occurred in the DBL (25.5 ng L$^{-1}$) and pore water of the sheet flow wetlands (7.4 ng L$^{-1}$) (Fig. 2 and Supporting information). In contrast, the lowest MeHg concentrations in water occurred among the impounded wetlands (0.14 ng L$^{-1}$ and 0.081 ng L$^{-1}$ for surface and pore water, respectively). Intermediate to these two ends of the spectrum were MeHg concentrations in the waters of the Freshwater-Influenced Bays (1.1 ng L$^{-1}$). Two-tailed t-tests (assuming unequal variances) demonstrated statistically significant differences between DBL and Freshwater-influenced Bays ($p < 5E-9$) and Sheetflow Wetland pore water ($P < 0.01$), as well as between DBL and Impounded Wetland surface water/pore water ($p < 9E-9$). The difference between Freshwater-influenced Bays/Sheetflow pore water and Impounded Wetland surface water/pore water settings was also statistically significant ($p < 0.007$).

The worldwide uncontaminated value for MeHg in water is 0.3 ng L$^{-1}$ (Gray and Hines, 2009), and this threshold is exceeded in the DBL, unfiltered Freshwater-influenced bays, and pore water of the Sheetflow wetlands. Naftz et al. (2009) observed mean MeHg

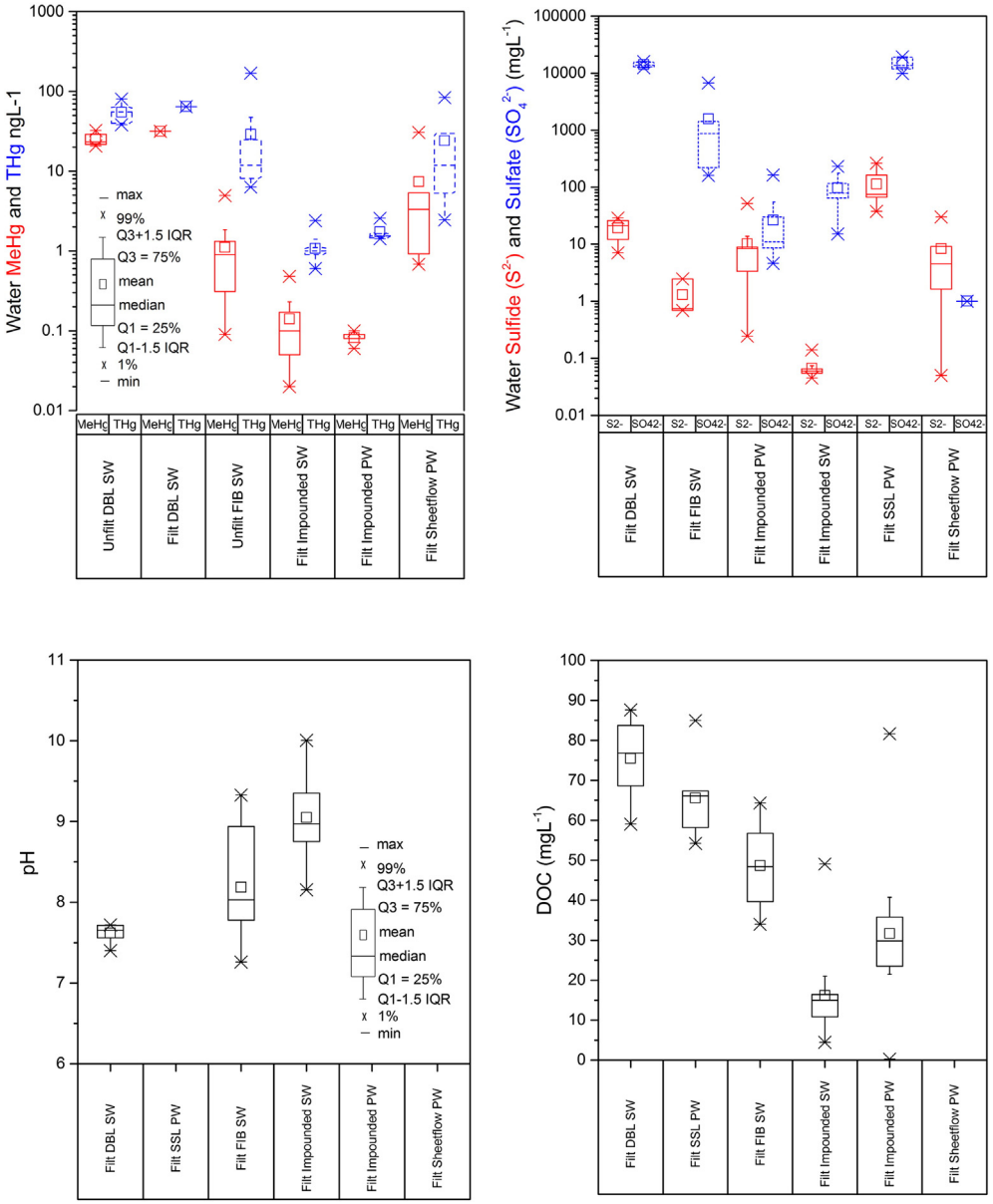


**Fig. 2.** Average water column MeHg, THg, sulfide, sulfate, DOC and pH across the freshwater to hypersaline continuum of the Great Salt Lake. SW = surface water, PW = pore water, Filt = filtered, Unfilt = unfiltered. Filtered DBL SW involves only two samples from a single site (A1). IQR = interquartile range = Q3–Q1. Blank values represent non-measured.

concentrations ranging 1–2 ng $L^{-1}$ in freshwater-influenced bays (in agreement with our results), and dissolved MeHg averaged and 1.2 ng $L^{-1}$ in the shallow brine layer overlying biostromes, and showed negligible spatial variation (Wurtsbaugh et al., 2011), four times the uncontaminated worldwide baseline of 0.3 ng $L^{-1}$ (Gray and Hines, 2009). Notably, the fraction of THg comprised by MeHg ranged approximately 30–80% in the DBL, and 20–50% in the Sheetflow wetland pore water (Fig. 2 and Supporting information), consistent with that fact that anoxic water within stratified systems can accumulate extremely high levels of THg and MeHg (Watras et al., 1995; Regnell et al., 1997). THg concentration differences among the settings mirrored those of MeHg, with mean THg concentrations equal to 55 ng $L^{-1}$ (DBL), 29 ng $L^{-1}$ (unfiltered Freshwater-influenced bays), 1.1 ng $L^{-1}$ (filtered Impounded Wetland surface water), 1.7 (filtered impounded wetland pore water), and 24 ng $L^{-1}$ (filtered Sheetflow pore water). The USEPA aquatic life standard for unfiltered THg is 12 ng $L^{-1}$ (USEPA, 1992), which was exceeded by the mean values in the DBL and Freshwater-Influenced bays, and was matched in the filtered Sheetflow pore water (Fig. 2). The worldwide uncontaminated value for THg in water is 2 ng $L^{-1}$ (Gray and Hines, 2009), which was exceeded in all settings except the filtered Impounded Wetland surface and pore waters (Fig. 2). Naftz et al. (2009) observed in limited samples among multiple sites mean THg concentrations ranging approximately 20 to 32 ng $L^{-1}$ in the DBL of the South Arm of GSL, and approximately 4 to 9 ng $L^{-1}$ in Freshwater-Influenced bays, in agreement with our results.

Across the continuum from freshwater to hypersaline settings, values for sulfate, sulfide, DOC and pH were bracketed within those for the freshwater wetlands at one end of the spectrum, and the hypersaline/anoxic DBL/SSL at the other end (Fig. 2 and Supporting information). The freshwater wetlands had the lowest sulfate (pore water ranging 5 to 160 mg $L^{-1}$), lowest sulfide (surface water ranging 0.04 to 0.2 mg $L^{-1}$), lowest DOC (surface water ranging 5 to 20 mg $L^{-1}$), and highest pH (surface water ranging 8–10). In contrast, the hypersaline anoxic DBL/SSL had the highest sulfate (DBL and SSL pore water ranging 12,000 to 20,000 mg $L^{-1}$), highest sulfide (SSL pore water ranging 37 to 63 mg $L^{-1}$), highest DOC (DBL and SSL pore water ranging 60 to 90 mg $L^{-1}$), and lowest pH (SSL pore water ranging 6.5 to 7.2) (Fig. 2 and Supporting information). Values of these parameters for other

settings were intermediate to the end-of-spectrum values given above. The high sulfate variability for freshwater-influenced bay site FBN3 (Fig. 2 and Supporting information) was due to a wind-driven brine wedge entering the causeway breach just north of that site during one of the sampling periods.

### 3.2. Sediment

THg and MeHg concentrations (dry weight) in sediment (from ambient non-incubated samples) were averaged across replicate samples and time series where available for given sites, and were averaged across sites within a given setting (Fig. 3). Figures, and a spreadsheet, providing specific sample locations and corresponding data within each setting are provided in the Supporting information. Across the continuum from freshwater to hypersaline settings, the highest mean MeHg concentrations in sediment occurred in the SSL (0.85 ng $g^{-1}$ dw) and Sheetflow wetlands (0.65 ng $g^{-1}$ dw), reflecting the preponderance of MeHg in water in the DBL and Sheetflow pore water. In contrast, mean sediment MeHg concentrations in the Freshwater-influenced bays (0.14 ng $g^{-1}$ dw) and Impounded Wetlands (0.11 ng $g^{-1}$ dw) were much lower. Mean THg concentrations were 103 ng $g^{-1}$ dw (SSL), 212 ng $g^{-1}$ dw (Sheetflow Wetlands), 56 ng $g^{-1}$ dw (Freshwater-influenced Bays), and 116 ng $g^{-1}$ dw (Impounded wetlands), showing far smaller variability relative to sediment MeHg across the freshwater-to- hypersaline continuum. Also shown in Fig. 3 are C and N concentrations for samples in which these constituents were measured, with the highest values being associated with the hypersaline open water sediments (SSL and Freshwater-influenced Bays). The marine sediment quality standard for THg is 410 ng $g^{-1}$ dw (State of Washington, 1995), which was not exceeded in any setting. Naftz et al. (2009) observed mean concentrations in GSL sediments ranging between approximately 90 and 260 ng $g^{-1}$ dw, in agreement with our data. Typical sediment MeHg/THg ratios are 1.0% to 1.5% according to Ullrich et al. (2001), which were not exceeded in any of the settings examined here.

### 3.3. Hg(II)-methylation

Values of $k_{meth}$ were variable even within any given setting in the continuum from freshwater to hypersaline (Fig. 4, Supporting information), ranging from 1E−6 to 1E−3 $h^{-1}$, but predominantly on the order of 5E−4 $h^{-1}$. These values are similar to other reported ranges, for example, values of $k_{meth}$ in sediments lakes and estuaries in sites in North America and Europe ranged from 0.01 to 0.05 $day^{-1}$ (4E−4 to 2E−3 $h^{-1}$) (Hintelman et al., 1995, 2000; Martın-Doimeadios et al., 2004; Heyes et al., 2006; Drott et al., 2008; Avramescu et al., 2011). Whereas incubation experiments were also performed to examine potential Hg(II) methylation rates in Freshwater-influenced bay surface water and the DBL, only the DBL showed significant Hg(II) methylation among water column incubations. Notably, SSL showed greater consistency of $k_{meth}$ values across season (April versus July) relative to the DBL (Fig. 4), suggesting that the SSL may be a more robust source of MeHg to the system relative to the DBL. Impounded wetlands as a group seem to show relatively low $k_{meth}$ values; however, the data are too limited to be conclusive.

Comparison of $k_{meth}$ values across multiple phases (SSL, sediment, DBL) and different locations is difficult because while rate constants provide an integrated measure of both microbial and abiotic Hg(II)-methylating and MeHg degrading processes, they are imperfect, as many processes are inherently lumped into a single 'apparent' rate constant. In particular, the inorganic Hg(II) reservoir (both the native pool and the isotope amendment) may not be fully available for microbial and abiotic Hg(II)-methylation reactions. The fraction of Hg(II) that is available is governed by many complex processes. For example, while $SO_4^{2-}$ reduction is most closely associated with methylation (Compeau and Bartha, 1985; Ranchou-Peyruse et al., 2009), high sulfide concentrations may inhibit methylation by reducing the bioavailability of complexed Hg(II) (Marvin-DiPasquale and Agee, 2003), depending on whether Hg is associated with dissolved versus nanoparticulate versus microparticulate sulfide (Gondikas et al., 2010; Zhang et al., 2012; Hsu-Kim et al., 2013; Gerbig et al., 2011). While there is no universally accepted method to measure biogoechemically available Hg(II), a number of approaches have been used, including selective extraction (Bloom et al., 2003; Yin et al., 2013), geochemical modeling (Benoit et al., 2001); chelation (Han et al., 2008), ethylation (Liang et al., 2013), and stannous chloride ($SnCl_2$) reduction (Miller et al., 2009). While debate continues as to the most appropriate approach (Liang et al., 2013), the methodologically-defined $SnCl_2$ reducible 'reactive' inorganic Hg ($Hg(II)_R$) assay has been successfully used in conjunction with $k_{meth}$ values derived from isotope amendment assays to calculate sediment MeHg production potential (MPP) rates, which were better correlated with in-situ MeHg concentrations than were $k_{meth}$ values alone

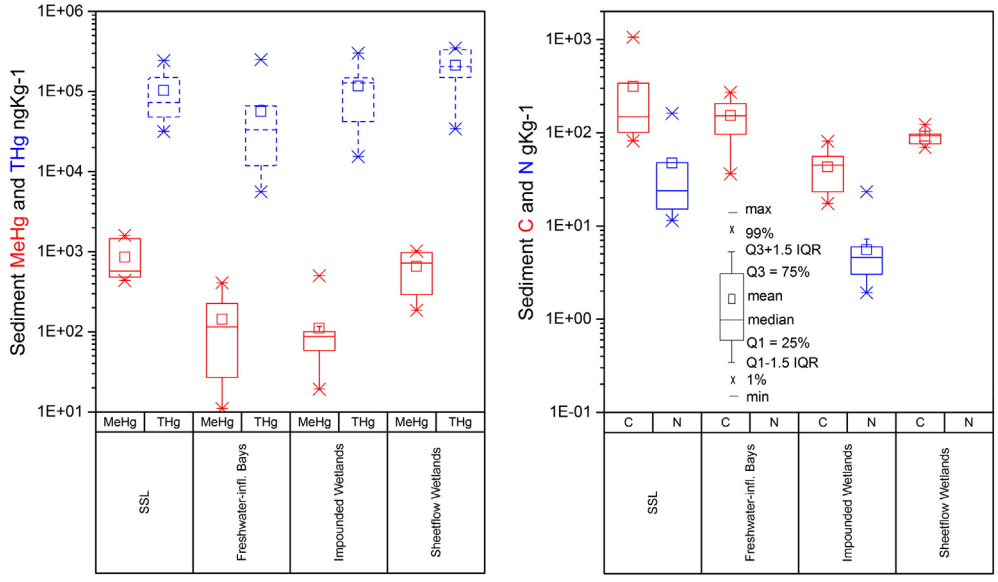


**Fig. 3.** Sediment and sediment slurry (SSL underlying DBL) MeHg, THg concentrations (ng $kg^{-1}$) and C,N concentrations (g $kg^{-1}$) (dry weight). IQR = interquartile range = Q3–Q1. Blank values represent non-measured.

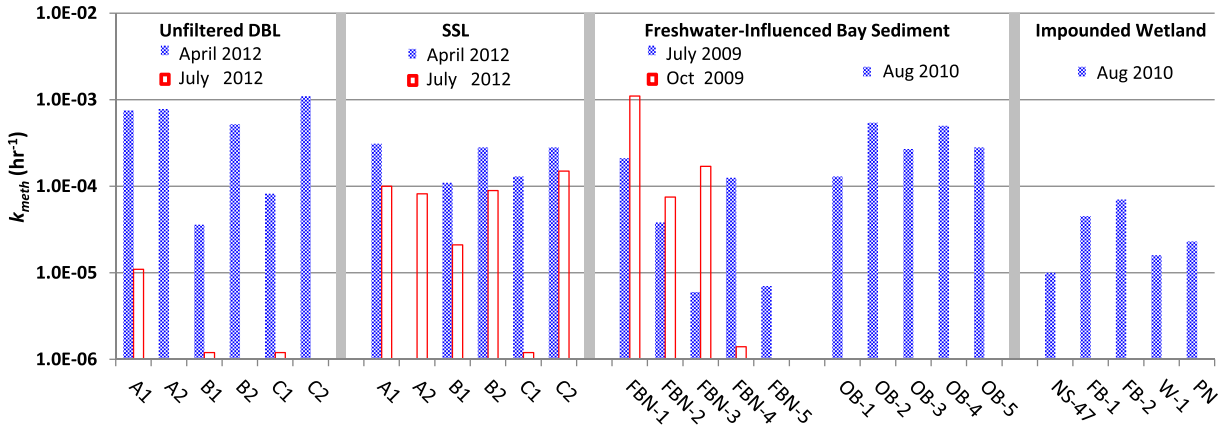


**Fig. 4.** Apparent first-order methylation rate constants ($k_{meth}$) in across the freshwater to hypersaline continuum. All values are from sediment slurries except for DBL. Blank values represent non-measured. Negligible values were substituted with 1.2E−6 ($h^{-1}$) (DBL B1 and C1, SSL C1) to differentiate from not measured.

(Marvin-DiPasquale et al., 2009a, 2014). The $Hg(II)_R$ proxy for the truly bioavailable Hg(II) pool has also proven extremely useful in ecosystem studies examining how changes in sediment geochemistry and redox conditions affect Hg(II) availability, and thus MeHg production (Windham-Myers et al., 2010; Marvin-DiPasquale et al., 2011, 2014).

$Hg(II)_R$ concentrations (wet weight basis) were generally lower in DBL relative to the underlying SSL (1.01 versus 58.2 ng $kg^{-1}$ ww, respectively, $p < 0.033$, using two-tailed t-test assuming equal variances) (Fig. 5, top), as expected from the lower solids content of DBL relative to SSL. $Hg(II)_R$ values (Fig. 5, top) were lower in July (open bars) relative to April (patterned bars) in the DBL (at the 0.05 level of significance via a two-sample t-test), and this temporal trend was also observed for $k_{meth}$ (Fig. 4). $Hg(II)_R$ concentrations in the SSL were relatively constant over time (equivalent July and April values at the 0.05 level of significance using a two-sample t-test) as was observed for $k_{meth}$ values. Methyl mercury production potential rates (MPP) (Fig. 5, bottom)

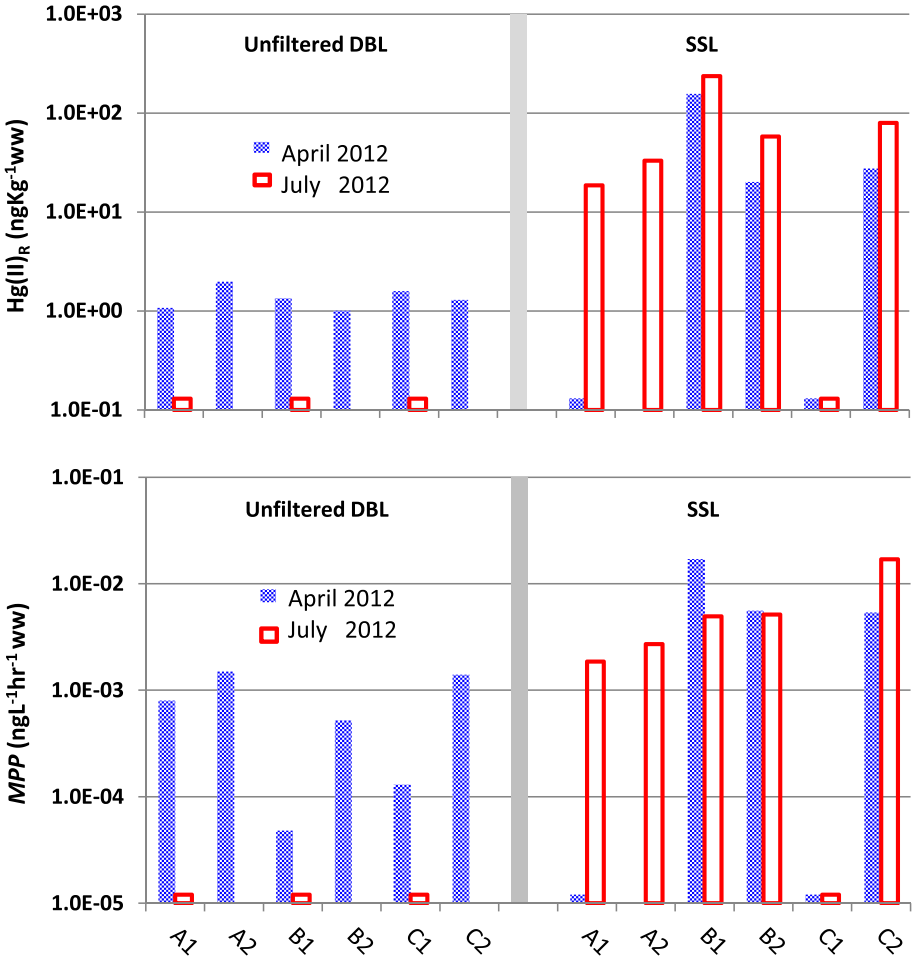


**Fig. 5.** April and July $Hg(II)_R$ concentrations and methylmercury production potentials (MPPs, time-integrated function of $k_{meth}$ and $Hg(II)_R$) for Deep Brine Layer (DBL) and underlying Sediment Slurry (SSL). SSL. $Hg(II)_R$ concentrations and MPPs expressed as wet weight rates for a more direct comparison with DBL. $Hg(II)_R$ values below detection limit were substituted with one-half the detection limit (SSL A1, C1 April 2012; DBL A1, B1, C1, and SSL C1 July 2012).

calculated as a function of $k_{meth}$ and $Hg(II)_R$ were dramatically lower in July (open bars) compared to April (patterned bars) in the DBL (at the 0.05 level using a two-sample t-test), and were relatively temporally consistent in the SSL relative to DBL (no difference at the 0.05 level). The temporal trends in MPP parallel the temporal trends seen in both the $Hg(II)_R$ concentrations (Fig. 5, top) and $k_{meth}$ values (Fig. 4), with the former reflecting Hg(II) bioavailability and the latter reflecting microbial activity. Because MPP rates in the SSL are temporally less dynamic and generally greater than those in the DBL, this suggests that the SSL may be responsible for a greater cumulative flux of MeHg into the system relative to the DBL, although additional work is needed to understand this possibility.

As a side note, comparison of MPPs in the SSL versus DBL could also be performed under the assumption that methylation is associated with particulates (i.e., reported as dry weight MPPs), or that areal extent of each phase is the critical point of comparison (reported as per area), as performed by Monperrus et al. (2007a). The former is common for sediment core-derived MPPs. However, the DBL and SSL are both water-dominated media (the dry weight % of SSL ranges from 23 to 39%, Supporting information), and their areal extents are equivalent (SSL being defined as directly below the DBL). Since our goal is to understand the relative significance of these two water-dominated phases regarding net production of MeHg in the GSL, we compared wet weight MPP values among those two phases.

MPPs measured in the SSL (expressed as dry weight) ranged from 0.0011 to 0.0572 (ng-kg$^{-1}$-h$^{-1}$ dry weight) (Supporting information), with a median and mean of 0.00495 and 0.00536, respectively. In comparison, MPP rates measured using the same approach in San Francisco Bay-Delta agricultural and freshwater wetland sediment, ranged from 0.012 to 20.4 (ng-kg$^{-1}$-h$^{-1}$ dry weight), with a median and mean MPP of 1.23 and 2.47 (ng-kg$^{-1}$-h$^{-1}$ dry weight), respectively (Marvin-DiPasquale et al., 2014). In a similarly conducted study of eight diverse streams from across the U.S.A., MPP rates ranged from <0.0001 to 3.78 (ng-kg$^{-1}$-h$^{-1}$ dry weight) across all streams, with individual stream medians ranging from 0.0065 to 0.393 (ng-kg$^{-1}$-h$^{-1}$ dry weight) (Marvin-DiPasquale et al., 2009a). Thus, MPPs from the DBL and SSL appear to correspond to the low end of the range exhibited in other settings, which suggests that the observed excess of MeHg in the DBL might reflect processes promoting its persistence rather than exceptional production. It should be noted that direct comparison of our MPPs to other reported "methylation potentials" (e.g., Furutani and Rudd, 1980; Kim et al., 2006; Han et al., 2007), even those focused on subsurface water (e.g., Korthals and Winfrey, 1987; Xun et al., 1987; Miskimmin et al., 1992; Mason et al., 1993; Monperrus et al., 2007b; Malcolm et al., 2010) is not useful since these studies considered $k_{meth}$ or % Hg(II) methylated as equivalent to methylation potential, and did not determine $Hg(II)_R$, or otherwise attempt to account for labile Hg(II).

The above findings suggest a possible persistence of MeHg in the DBL. Among factors that potentially act to stabilize MeHg in the DBL are: salinity (Black et al., 2012; Zhang et al., 2012), light attenuation (Black et al., 2012), and complexation with dissolved organic matter (Zhong and Wang, 2009; Dong et al., 2010; Hsu-Kim et al., 2013) and other moieties such as sulfide (Hintelmann et al., 1997; Zhong and Wang, 2009). Light is absent in the DBL due to absorption in the algae-rich upper brine layer and high concentrations of dissolved and particulate organic matter in the DBL (Diaz et al., 2009). Field measurements made in July 2013 (LiCor model LI-193SA spherical quantum sensor) showed that photosynthetically active radiation (PAR) decreased from 2000 to 131 μmol-s$^{-1}$-m$^{-1}$ from the lake surface to the top of the DBL (6.5 m depth), with additional decrease to 4.7 μmol-s$^{-1}$-m$^{-1}$ at 7 m depth (Supporting information), well above the maximum ~9 m depth of the DBL.

### 3.4. Correlations

THg was positively power-law correlated to MeHg in filtered surface and pore water, but not unfiltered samples (Freshwater-influenced Bay samples) (Fig. 6), indicating (as expected) that particulate (>0.45 μm) fractions of Hg are not in chemical equilibrium with dissolved fractions. A power-law correlation was examined (Excel 2010) in order to examine the relationship across the several-log range in concentrations across the range of settings. In linear space the correlation was [MeHg] = 0.4015[THg] − 0.5571 ($r^2$ = 0.95). Unfiltered DBL samples also fell within the MeHg-THg correlation, likely because MeHg in DBL is overwhelmingly in the <0.45 μm size fraction. In replicate samples from DBL site A1 (Fig. 2 and Supporting information), comparison of filtered and unfiltered samples shows that 61% of THg was in the <0.45 μm size fraction (106 ± 0.54 ng-L$^{-1}$ unfiltered, 64.4 ± 1.93 ng-L$^{-1}$ filtered) and 92% of MeHg was in the <0.45 μm size fraction (34.2 ± 0.87 ng-L$^{-1}$ unfiltered, 31.6 ± 1.15 ng-L$^{-1}$ filtered). Whereas A1 is only one site in the DBL, it is likely representative, as demonstrated by highly consistent results for a suite of trace elements at three sites spanning the DBL (Supporting information). That 61% of THg in the DBL lies within the <0.45 μm size fraction is a distinct contrast to the more common observation such as in the Impounded freshwater wetlands, where THg is predominantly associated (>90%) with the >0.45 μm fraction (e.g., Carling et al., 2011, 2013). Notably, Diaz et al. (2009), showed using flow field flow fractionation that Hg in the DBL is associated with macromolecule-sized moieties (<3 nm).

Dissolved sulfate showed positive power-law correlation with MeHg in unfiltered and filtered surface and pore water samples (Supporting information), although this relationship was significant for the combined set of samples only, and was not significant for any single aquatic compartment (unfiltered DBL, unfiltered freshwater-influenced bay surface water, filtered wetland surface water, filtered wetland pore water). DOC also showed positive log-linear correlation with MeHg in unfiltered and filtered surface water (excluding pore water) (Supporting information), but again the correlation was not significant within any single aquatic compartment. There was a lack of correlation between MeHg and sulfide, pH, and Cl (as a proxy for salinity) in water, as well as between MeHg and THg in sediment (Supporting information). Ratios such as MeHg/THg or sulfide/sulfate did not improve correlations, and greatly weakened them in the case of sulfide/sulfate because of the large range of sulfate concentrations within the system.

Correlations between $k_{meth}$ values and all other parameters were significant only for sediment organic matter content (positive) in the freshwater influenced bays and impounded wetlands, as has been previously reported in other settings (e.g., Lambertsson and Nilsson, 2006; Marvin-DiPasquale et al., 2009a), and likely reflects the stimulatory influence of organic matter on overall microbial activity. The $k_{meth}$ values for two of the freshwater influenced bay transects (FBN summer, OB summer) and the impounded wetlands were significantly correlated ($P < 0.05$) to sediment organic matter content (Fig. 7), with $r^2$ values of 0.90, 0.67, and 0.82, respectively. The corresponding 90% confidence intervals are provided for FBN summer, OB summer, and the impounded wetlands in Fig. 7. The FBN fall correlation had a relatively

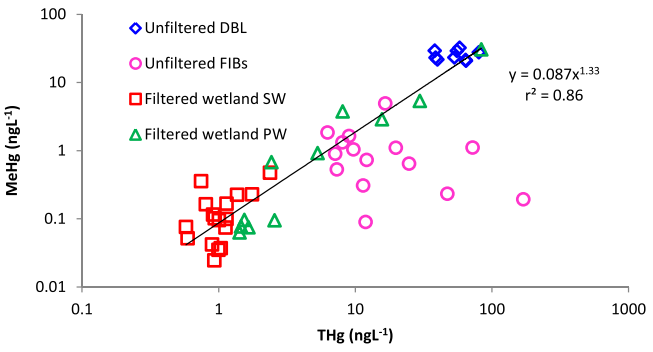


**Fig. 6.** Surface and pore water MeHg versus THg concentrations. SW = surface water, PW = pore water. Trendline reflects combined data from filtered PW samples.

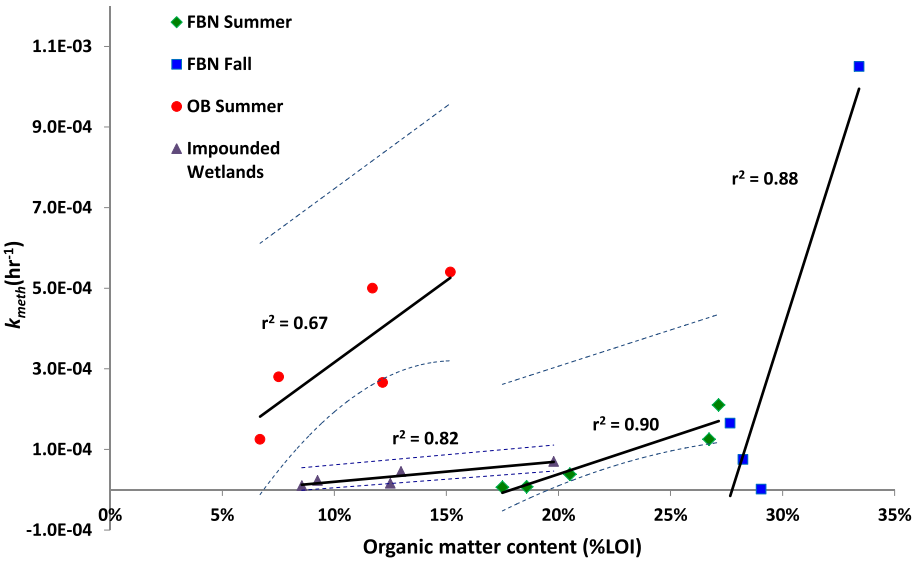


**Fig. 7.** Scatter plots of methylation rate constants ($k_{meth}$) ($h^{-1}$) vs. percent sediment organic matter content (%LOI) in sediment from the freshwater bays (summer and fall 2009) and impounded wetlands (summer 2011) with trend lines and $r^2$. Dashed lines represent 90% confidence intervals.

high $r^2$ of 0.88 but this correlation results from a single outlier, and is not statistically significant with $P > 0.05$ ($P = 0.06$).

The $K_{meth}$-OM correlations suggest an important role of sediment organic matter in regulating the production of MeHg in the freshwater influenced bays and impounded wetlands. However, when $k_{meth}$ from the various transects of the freshwater influenced bays examined here are grouped together, the correlation disappears, indicating that other factors in addition to sediment organic matter content (e.g., possibly organic matter lability, sulfide concentrations, among others) influence $k_{meth}$. Whereas there was no correlation between $Hg(II)_R$ and DOC in the DBL or in SSL pore water, nor between $Hg(II)_R$ and sulfide in the DBL, there was significant inverse correlation ($r^2 = 0.89$) between $Hg(II)_R$ and sulfide in SSL pore water (Fig. 8). This is similar to the negative relationship reported between $Hg(II)_R$ and solid phase reduced sulfur pools reported in other studies (Marvin-DiPasquale et al., 2009a,b, 2014) and is consistent with the assertion that $Hg(II)_R$ serves as a reasonable proxy for the pool of Hg(II) most readily available for methylation, the rationale being that Hg(II) bound to sulfides is less available for $SnCl_2$ reduction and microbial Hg(II) methylation.

### 3.5. Spatial correspondence

The measured concentrations highlight the DBL and SSL, as well as the Sheetflow wetlands, as locations having exceptional MeHg concentrations and MeHg/THg ratios in water relative to other areas of the GSL (Figs. 2 and 3). The DBL, SSL, Sheetflow wetlands, and Impounded wetlands each have elevated sulfide concentrations; whereas the Impounded wetlands lack elevated MeHg (Fig. 2). DOC is exceptional among the DBL and SSL, but not among the other settings (Fig. 2). The spatial constancy of the elevated MeHg concentrations within the DBL is notable given the large area it encompassed within the GSL aquatic system during the study (Fig. 2). The findings suggest that elevated Hg concentrations in avian species at Stansbury Island relative to Antelope Island (described above) may reflect closer proximity of Stansbury Island to the elevated MeHg concentrations in the DBL relative to lower-MeHg concentration Freshwater-influenced bays. However, connection of elevated MeHg in the DBL to elevated Hg in biota is not proven. The recent finding of high Hg concentrations in spiders (ranging ~500 to 2100 mg $kg^{-1}$ dw) sampled from two shoreline locations on Antelope Island in 2012 (Frank Black, personal communication) suggests a potential connection between aquatic invertebrates (e.g., brine flies) and terrestrial invertebrates at the shoreline.

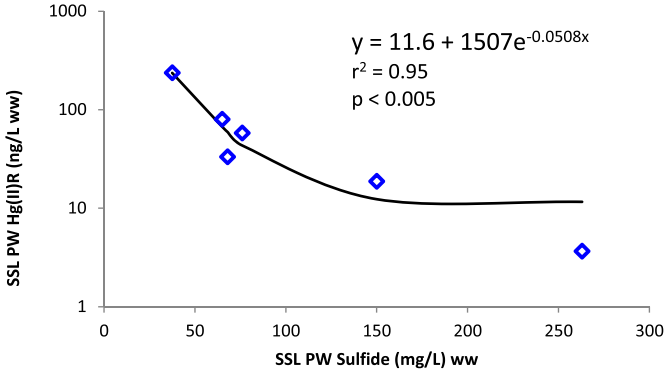


**Fig. 8.** Correlation of $Hg(II)_R$ to sulfide in SSL pore water, both constituent concentrations expressed as wet weight.

### 3.6. Temporal correspondence

Water column MeHg concentrations showed no clear temporal trend. In contrast, SSL and sediment MeHg concentrations indicated a weak overall decreasing trend from April to September in 2012 (Supporting information). This possible temporal dynamic in sediment MeHg concentrations warrants additional investigation because it may influence inter-annual dynamics of Hg accumulation in the ecosystem. An important temporal trend identified in the Hg(II) methylation rate measurements ($k_{meth}$ and MPP) is the reduced rate of methylation in the DBL that occurs during mid-summer (July), since it appears to correspond to the reduced Hg burden in aquatic invertebrates (described above). This apparent correspondence in timing is intriguing because there is a potential connection of MeHg in the DBL to aquatic invertebrates in the shallow brine layer via the observed and expected entrainment of DBL into overlying water (described above). The factors driving the timing of increased Hg(II) methylation rates in the DBL and increases Hg burdens in aquatic invertebrates are unknown, but may be related to labile nutrient and carbon delivery during spring snowmelt runoff (as suggested by the observed higher potential Hg(II) methylation rates during April), among other possibilities.

## 4. Conclusions

The results herein identify noteworthy areas of elevated MeHg concentrations (particularly the DBL and SSL of the GSL, and the Sheetflow wetlands) and Hg(II) methylation (DBL and SSL). Data suggest persistence (rather than exceptional production) as the reason for high MeHg concentrations in the DBL. Results demonstrate widespread spatial constancy of elevated MeHg in the DBL of the open water GSL system, which is the most proximal aquatic setting to the area where elevated Hg burdens in avian species were previously reported to be highest. Results demonstrate reduced Hg(II) methylation rates in the DBL during mid-summer (July), which corresponds to the time during which reported Hg burdens in aquatic invertebrates (brine shrimp and brine flies) were lowest according to multiple studies. These spatial and temporal correspondences suggest a connection between elevated Hg in biota and elevated Hg in the DBL, and therefore warrant further investigation into the role of the DBL in Hg propagation into the GSL ecosystem.

## Acknowledgments

This research was supported by funding from the Division of Forestry, Fire, and State Lands (FFSL) of the Utah Department of Natural Resources, Jordan River/Farmington Bay Water Quality Council, and Central Davis Sewer District. Additionally, we would like to thank Michelle Arias (USGS, Menlo Park) for $Hg(II)_R$ assays and Brooks Rand LLC for technical support. We owe a great deal of thanks to Marissa Taddie who developed the ring plots provided in the Supporting information. We greatly appreciate the highly effective comments of several anonymous reviewers.

## Appendix A. Supplementary data

Supplementary data to this article include comprehensive ring plots linking data directly to physiographic setting, detailed methods with quality assurance, tabular information regarding spike concentrations, correlation plots not shown in main text, kinetic fits to isotope data for methylation rate constants. A spreadsheet with all data is provided.

Supplementary data associated with this article can be found in the online version, at http://dx.doi.org/10.1016/j.scitotenv.2014.12.092. These data include Google map of the most important areas described in this article.

## References

Aldrich, T.W., Paul, D.S., 2002. Avian ecology of Great Salt Lake. In: Gwynn, J.W. (Ed.), Great Salt Lake: An Overview of Change. Utah Department of Natural Resources Special Publication.

Avramescu, M.L., Yumvihoze, E., Hintelmann, H., Ridal, J., Fortin, D., Lean, D.R.S., 2011. Biogeochemical factors influencing net mercury methylation in contaminated freshwater sediments from the St. Lawrence River in Cornwall, Ontario, Canada. Sci. Total Environ. 409, 968–978. http://dx.doi.org/10.1016/j.scitotenv.2010.11.016.

Baeyens, W., Leermakers, M., Papina, T., Saprykin, A., Brion, N., Noyen, J., De Gieter, M., Elskens, M., Goeyens, L., 2003. Bioconcentration and biomagnification of mercury and methylmercury in North Sea and Scheldt estuary fish. Arch. Environ. Contam. Toxicol. 45, 498–508.

Baskin, R.L., 2005. Calculation of area and volume for the south part of the Great Salt Lake. US Geological Survey Open-File Report 2005–1327. US Department of Interior, Utah.

Beisner, K., Naftz, D.L., Johnson, W.P., Diaz, X., 2009. Selenium and trace element mobility affected by periodic displacement of stratification in the Great Salt Lake, Utah. Sci. Total Environ. 407, 5263–5273. http://dx.doi.org/10.1016/j.scitotenv.2009.06.005.

Benoit, J.M., Gilmour, C.C., Mason, R.P., 2001. The influence of sulfide on solid-phase mercury bioavailability for methylation by pure cultures of *Desulfobulbus propionicus* (1pr3). Environ. Sci. Technol. 35 (1), 127–132.

Black, F.J., Poulin, B.A., Flegal, A.R., 2012. Factors controlling the abiotic photo-degradation of monomethylmercury in surface waters. Geochim. Cosmochim. Acta 84, 492–507.

Bloom, N.S., Colman, J.A., Barber, L., 1997. Artifact formation of methyl mercury during aqueous distillation and alternative techniques for the extraction of methyl mercury from environmental samples. Fresenius J. Anal. Chem. 358, 371–377.

Bloom, N.S., Preus, E., Katon, J., Hiltner, M., 2003. Selective extractions to assess the biogeochemically relevant fractionation of inorganic mercury in sediments and soils. Anal. Chim. Acta. 479 (2), 233–248.

Carling, G.T., Fernandez, D.P., Rudd, A., Pazmino, E., Johnson, W.P., 2011. Trace element diel variations and particulate pulses in perimeter freshwater wetlands of Great Salt Lake, Utah. Chem. Geol. 283, 87–98.

Carling, G.T., Richards, D.C., Hoven, H., Miller, T., Fernandez, D.P., Rudd, A., Pazmino, E., Johnson, W.P., 2013. Relationships of surface water, pore water, and sediment chemistry in wetlands adjacent to Great Salt Lake, Utah, and potential impacts on plant community health. Sci. Total Environ. 443, 798–811.

Chin, Y.P., Traina, S.J., Swank, C.R., Backhus, D., 1998. Abundance and properties of dissolved organic matter in pore waters of a freshwater wetland. Limnol. Oceanogr. 43, 1287–1296.

Choi, S.C., Bartha, R., 1994. Environmental factors affecting mercury methylation in estuarine sediments. Bull. Environ. Contam. Toxicol. 53, 805–812.

Cline, C., Neill, J., Whitehead, J., Gardberg, J., January, 2011. Mercury concentrations in cinnamon teal (*Anas cyanoptera*) and northern shoveler (*Anas clypeata*) at Great Salt Lake, Utah in Ecosystem Assessment of Mercury in the Great Salt Lake, Utah, 2008. Report for Utah Department of Environmental Quality Division of Water Quality.

Compeau, G.C., Bartha, R., 1985. Sulfate-reducing bacteria: principal methylators of mercury in anoxic estuarine sediment. Appl. Environ. Microbiol. 50, 498–502.

Conover, M.R., Vest, J.L., 2009. Concentrations of selenium and mercury in eared grebes (*Podiceps nigricollis*) from Utah's Great Salt Lake, USA. Environ. Toxicol. Chem. 28, 1319–1323.

Diaz, X., Johnson, W.P., Fernandez, D., Naftz, D.L., 2009. Size and elemental distributions of nano- to micro-particulates in the geochemically-stratified Great Salt Lake. Appl. Geochem. 24, 1653–1665.

Dicataldo, G., Hayes, D.F., Johnson, W.P., Moellmer, W.O., Miller, T., 2010. Effect of dissolved oxygen, pH, and water temperature on diel changes of dissolved selenium and other trace metals in a Great Salt Lake wetland. Appl. Geochem. 26, 28–36. http://dx.doi.org/10.1016/j.apgeochem.2010.10.011.

Dong, W., Liang, L., Brooks, S., Southworth, G., Gu, B., 2010. Roles of dissolved organic matter in the speciation of mercury and methylmercury in a contaminated ecosystem in Oak Ridge, Tennessee. Environ. Chem. 7, 94–102.

Drott, A., Lambertsson, L., Bjorn, E., Skyllberg, U., 2008. Do potential methylation rates reflect accumulated methyl mercury in contaminated sediments? Environ. Sci. Technol. 42 (1), 153–158.

Furutani, A., Rudd, J.W.M., 1980. Measurement of mercury methylation in lake water and sediment samples. Appl. Environ. Microbiol. 40, 770–776.

Gerbig, C.A., Kim, C.S., Stegemeier, J.P., Ryan, J.N., Aiken, G.R., 2011. Formation of nanocolloidal metacinnabar in mercury-DOM-sulfide systems. Environ. Sci. Technol. 45, 9180–9187.

Gilmour, C.C., Riedel, G.S., Ederington, M.C., Bell, J.T., Benoit, J.M., Gill, G.A., Stordal, M.C., 1998. Methylmercury concentrations and production rates across a trophic gradient in the northern Everglades. Biogeochemistry 40, 327–345.

Gondikas, A.P., Jang, E.K., Hsu-Kim, H., 2010. Influence of amino acids cysteine and serine on aggregation kinetics of zinc and mercury sulfide colloids. J. Colloid Interface Sci. 347, 167–171.

Graham, A.M., Aiken, G.R., Gilmour, C.C., 2012. Dissolved organic matter enhances microbial mercury methylation under sulfidic conditions. Environ. Sci. Technol. 46, 2715–2723.

Gray, J.E., Hines, M.E., 2009. Biogeochemical mercury methylation influenced by reservoir eutrophication, Salmon Falls Creek Reservoir, Idaho, USA. Chem. Geol. 258, 157–167.

Gwynn, J.W., 2002. Great Salt Lake: chemical and physical variations of the brine and effects of the 2013SPRR causeway, 1966–1996. In: Gwynn, J.W. (Ed.), Great Salt Lake: An Overview of Change. Utah Department of Natural Resources Special Publication.

Han, S., Obraztsova, A., Pretto, P., Choe, K.Y., Gieskes, J., Deheyn, D.D., Tebo, B.M., 2007. Biogeochemical factors affecting mercury methylation in sediments of the Venice Lagoon, Italy. Environ. Toxicol. Chem. 26, 655–663.

Han, F.X., Shiyab, S., Chen, J., Su, Y., Monts, D.L., Waggoner, C.A., Matta, F.B., 2008. Extractability and bioavailability of mercury from a mercury sulfide contaminated soil in Oak Ridge, Tennessee, USA. Water Air Soil Pollut. 194 (1–4), 67–75.

Heyes, A., Mason, R.P., Kim, E.H., Sunderland, E., 2006. Mercury methylation in estuaries: insights from using measuring rates using stable mercury isotopes. Mar. Chem. 102 (1–2), 134–147.

Hintelman, H., Evans, D., Villeneuve, J.Y., 1995. Measurement of mercury methylation in sediments by using enriched stable mercury isotopes combined with methylmercury determination by gas chromatography-inductively coupled plasma mass spectrometry. J. Anal. At. Spectrom. 10, 619–624.

Hintelman, H., Keppel-Jones, K., Evans, R.D., 2000. Constants of mercury methylation and demethylation rates in sediments and comparison of tracer and ambient mercury availability. Environ. Toxicol. Chem. 10 (9), 2204–2211.

Hintelmann, H., Evans, R.D., 1997. Application of stable isotopes in environmental tracer studies — measurement of monomethylmercury ($CH_3Hg+$) by isotope dilution ICP-MS and detection of species transformation. Fresenius J. Anal. Chem. 358, 378–385.

Hintelmann, H., Welbourn, P.M., Evans, R.D., 1997. Measurement of complexation of methylmercury(II) compounds by freshwater humic substances using equilibrium dialysis. Environ. Sci. Technol. 31, 489–495.

Hsu-Kim, H., Kucharzyk, K.H., Zhang, T., Deshusses, M.A., 2013. Mechanisms regulating mercury bioavailability for methylating microorganisms in the aquatic environment: a critical review. Environ. Sci. Technol. 47, 2441–2456.

Ingvorsen, K., Brandt, K.K., 2002. Anaerobic microbiology and sulfur cycling in hypersaline sediments with special reference to Great Salt Lake. In: Gwynn, J.W. (Ed.), Great Salt Lake: an overview of change. Utah Department of Natural Resources Special Publication.

Kim, E.H., Mason, R.P., Porter, E.T., Soulen, H.L., 2006. The impact of resuspension on sediment mercury dynamics, and methylmercury production and fate: a mesocosm study. Mar. Chem. 102, 300–315.
King, J.K., Kostka, J.E., Frischer, M.E., Saunders, F.M., 2000. Sulfate-reducing bacteria methylate mercury at variable rates in pure culture and in marine sediments. Appl. Environ. Microbiol. 66, 2430–2437.
Korthals, E.T., Winfrey, M.R., 1987. Seasonal and spatial variations in mercury methylation and demethylation in an oligotrophic lake. Appl. Environ. Microbiol. 53, 2397–2404.
Lambertsson, L., Nilsson, M., 2006. Organic material: the primary control on mercury methylation and ambient methyl mercury concentrations in estuarine sediments. Environ. Sci. Technol. 40, 1822–1829.
Liang, L., Horvat, M., Alvarez, J., Young, L., Kotnik, J., Zhang, L., 2013. The challenge and its solution when determining biogeochemically reactive inorganic mercury (RHg): getting the analytical method right. Am. J. Anal. Chem. 4, 623–632. http://dx.doi.org/10.4236/ajac.2013.411074.
Loving, B.L., Waddell, K.M., Miller, C.W., 2002. Water and salt balance of Great Salt Lake, Utah, and simulation of water and salt movement through the causeway, 1963–98. In: Gwynn, J.W. (Ed.), Great Salt Lake: An Overview of Change. Utah Department of Natural Resources Special Publication.
Malcolm, E.G., Schaefer, J.K., Ekstrom, E.B., Tuit, C.B., Jayakumar, A., Park, H., Ward, B.B., Morel, F.M.M., 2010. Mercury methylation in oxygen deficient zones of the oceans: no evidence for the predominance of anaerobes. Mar. Chem. 122, 11–19.
Martın-Doimeadios, R.C.R., Tessier, E., Amouroux, D., Guyoneaud, R., Duran, R., Caumette, P., Donard, O.F.X., 2004. Mercury methylation/demethylation and volatilization pathways in estuarine sediment slurries using species-specific enriched stable isotopes. Mar. Chem. 90, 107–123.
Marvin-DiPasquale, M., Agee, J., 2003. Microbial mercury cycling in sediments of the San Francisco Bay-Delta. Estuaries 26, 1517–1528.
Marvin-DiPasquale, M., Cox, M.H., 2007. Legacy mercury in Alviso Slough, South San Francisco Bay, California: concentration, speciation and mobility. U.S. Geological Survey Open-File Report 2007–1240.
Marvin-DiPasquale, M., Agee, J., Bouse, R., Jaffe, B., 2003. Microbial cycling of mercury in contaminated pelagic and wetland sediments of San Pablo Bay, California. Environ. Geol. 43, 260–267.
Marvin-DiPasquale, M., Lutz, M.A., Krabbenhoft, D.P., Aiken, G.R., Orem, W.H., Hall, B.D., DeWild, J.F., Brigham, M.E., 2008. Total mercury, methylmercury, methylmercury production potential, and ancillary streambed-sediment and pore-water data for selected streams in Oregon, Wisconsin, and Florida, 2003–04. U.S. Geological Survey, Reston, VA (Data Series 375).
Marvin-DiPasquale, M., Lutz, M.A., Brigham, M.E., Krabbenhoft, D.P., Aiken, G.R., Orem, W.H., Hall, B.D., 2009a. Mercury cycling in stream ecosystems. 2. Benthic methylmercury production and bed sediment-pore water partitioning. Environ. Sci. Technol. 43, 2726–2732.
Marvin-DiPasquale, M., Alpers, C.N., Fleck, J.A., 2009b. Mercury, methylmercury, and other constituents in sediment and water from seasonal and permanent wetlands in the Cache Creek Settling Basin and Yolo Bypass, Yolo County, California, 2005–06. U.S. Geological Survey Open File Report 2009–1182 (69 pp.).
Marvin-DiPasquale, M., Agee, J.L., Kakouros, E., Kieu, L.H., Fleck, J.A., Alpers, C.N., 2011. The effects of sediment and mercury mobilization in the South Yuba River and Humbug Creek confluence area, Nevada County, California: Concentrations, speciation and environmental fate — part 2: laboratory experiments. U.S. Geological Survey Open-File Report 2010-1325B (January).
Marvin-DiPasquale, M., Windham-Myers, L., Agee, J.L., Kakouros, E., Kieu, L.H., Fleck, J., Alpers, C.N., Stricker, C., 2014. Methylmercury production in sediment from agricultural and non-agricultural wetlands in the Yolo Bypass, California. Sci. Total Environ. 484, 288–299.
Mason, R.P., Fitzgerald, W.F., Hurley, J., Hanson, A.K., Donaghay, P.L., Sieburth, J.M., 1993. Mercury biogeochemical cycling in a stratified estuary. Limnol. Oceanogr. 38, 1227–1241.
Mason, R.P., Heyes, D., Sveinsdottir, A., 2006. Methylmercury concentrations in fish from tidal waters of the Chesapeake Bay. Arch. Environ. Contam. Toxicol. 51, 425–437.
Miller, C.L., Southworth, G., Brooks, S., Liang, L., Gu, B., 2009. Kinetic controls on the complexation between mercury and dissolved organic matter in a contaminated environment. Environ. Sci. Technol. 43, 8548–8553.
Miskimmin, B.M., Rudd, J.W.M., Kelly, C.A., 1992. Influence of dissolved organic carbon, pH, and microbial respiration rates on mercury methylation and demethylation in lake water. Can. J. Fish. Aquat. Sci. 49, 17–22.
Monperrus, M., Tessier, E., Point, D., Vidimova, K., Amouroux, D., Guyoneaud, R., Leynaert, A., Grall, J., Chauvaud, L., Thouzeau, G., Donard, O.F.X., 2007a. The biogeochemistry of mercury at the sediment-water interface in the Thau Lagoon. 2. Evaluation of mercury methylation potential in both surface sediment and the water column. Estuar. Coast. Shelf Sci. 72, 485–496.
Monperrus, M., Tessier, E., Amouroux, D., Leynaert, A., Huonnic, P., Donard, O., 2007b. Mercury methylation, demethylation and reduction rates in coastal and marine surface waters of the Mediterranean Sea. Mar. Chem. 107, 49–63.
Naftz, D., Angeroth, C., Kenney, T., Waddell, B., Darnall, N., Silva, S., Perschon, C., Whitehead, J., 2008. Anthropogenic influences on the input and biogeochemical cycling of nutrients and mercury in Great Salt Lake, Utah, USA. Appl. Geochem. 23, 1731–1744.
Naftz, D., Fuller, C., Cederberg, J., Krabbenhoft, D., Whitehead, J., Gardberg, J., Beisner, K., 2009. Mercury inputs to Great Salt Lake, Utah: reconnaissance-phase results. In: Oren, D. Naftz, Palacios, P., Wurtsbaugh, W.A. (Eds.), Saline Lakes Around the World: Unique Systems with Unique Values. Natural Resources and Environmental Issues. S.J. and Jessie Quinney Natural Resources Research Library, pp. 37–49.
Peterson, C., Gustin, M., 2008. Mercury in the air, water, and biota at the Great Salt Lake (Utah, USA). Sci. Total Environ. 405, 255–268.
Ranchou-Peyruse, M., Monperrus, M., Bridou, R., Duran, R., Amouroux, D., Salvado, J.C., Guyoneaud, R., 2009. Overview of mercury methylation capacities among anaerobic bacteria including representatives of the sulphate-reducers: implications for environmental studies. Geomicrobiol J. 1, 1–8.
Regnell, O., Ewald, G., Lord, E., 1997. Factors controlling temporal variation in methyl mercury levels in sediment and water in a seasonally stratified lake. Limnol. Oceanogr. 42, 1784–1795. http://dx.doi.org/10.4319/lo.1997.42.8.1784.
Scholl and Ball, 2005. An evaluation of mercury concentrations in waterfowl from the Great Salt Lake, Utah for 2004 and 2005 Health Evaluation. Utah Department of Health Office of Epidemiology Environmental Epidemiology Program.
Scholl and Ball, 2006. An evaluation of mercury concentrations in waterfowl from the Great Salt Lake, Utah for 2005 and 2006 Health Evaluation. Utah Department of Health Office of Epidemiology Environmental Epidemiology Program.
State of Washington, 1995. Marine sediment quality standards. http://apps.leg.wa.gov/WAC/default.aspx?cite=173-204-320 (accessed on June 3, 2010).
Sunderland, E.M., Gobas, F.P.A.C., Branfireun, B.A., Heyes, A., 2006. Environmental controls on the speciation and distribution of mercury in coastal sediments. Mar. Chem. 102, 111–123.
Ullrich, S.M., Tanton, T.W., Abdrashitova, S.A., 2001. Mercury in the aquatic environment: a review of factors affecting methylation. Crit. Rev. Environ. Sci. Technol. 31, 241–293.
USEPA, 1992. Water quality standards; establishment of numeric criteria for priority toxic pollutants; states' compliance; final rule, Federal Register. 40 CFR Part 131, 57/246. U.S. Environmental Protection Agency, pp. 60847–60916.
USEPA, 2000. Guidance for assessing chemical contaminant data for use in fish advisories. 3rd ed Fish Sampling and Analysis vol. 1. Publication No. EPA 823-B-00-007, Washington.
USEPA Method 1630, 2001. Methylmercury in Water by Distillation, Aqueous Ethylation, Purge and Trap, and CVAFS. U.S. Environmental Protection Agency.
USEPA Method 1631, 2001. (Appendix): Appendix to Method 1631: Total Mercury in Tissue, Sludge, Sediment, and Soil by Acid Digestion and BrCl Oxidation. U.S. Environmental Protection Agency.
USEPA Method 1631, 2002. Revision E: Mercury in Water by Oxidation, Purge and Trap, and Cold Vapor Atomic Fluorescence Spectrometry. U.S. Environmental Protection Agency.
USEPA Method 1684, 2001. Total, Fixed, and Volatile Solids in Water, Solids, and Biosolids. U.S. Environmental Protection Agency.
USEPA Method 200.8, 1994. Revision 5.4: Determination of Trace Elements in Waters and Wastes by Inductively Coupled Plasma-mass Spectrometry. U.S. Environmental Protection Agency.
Van Leeuwen, J., Brown, P., Butler, J., Whitehead, J., Gardberg, J., 2011. Chapter 2: assessment of total mercury concentrations in Great Salt Lake Artemia (Artemia Franciscana) in ecosystem assessment of mercury in the Great Salt Lake, Utah 2008. report for Utah Department of Environmental Quality Division of Water Quality (January).
Vest, J.L., Conover, M.R., Perschon, C., Luft, J., Hall, J.O., 2008. Trace Element Concentrations in Wintering Waterfowl from the Great Salt Lake. Utah Arch. Environ. Contam, Toxicol http://dx.doi.org/10.1007/s00244-008-9184-8.
Watras, C.J., Bloom, N.S., Claas, S.A., Morrison, K.A., Gilmour, C.C., Craig, S.R., 1995. Methylmercury production in the anoxic hypolimnion of a dimictic seepage lake. Water Air Soil Pollut. 80, 735–745. http://dx.doi.org/10.1007/BF01189725.
Windham-Myers, L., Marvin-Dipasquale, M., Krabbenhoft, D.P., Agee, J.L., Cox, M.H., Heredia-Middleton, P., Coates, C., Kakouros, E., 2010. Experimental removal of wetland emergent vegetation leads to decreased methylmercury production in surface sediment. J. Geophys. Res. Biogeosci. 114. http://dx.doi.org/10.1029/2008JG000815.
Wurtsbaugh, W.W., Gardberg, J., Izdepski, C., 2011. Biostrome communities and mercury and selenium bioaccumulation in the Great Salt Lake (Utah, USA). Sci. Total Environ. 409, 4425–4434.
Xun, L., Campbell, N.E.R., Rudd, J.W.M., 1987. Measurements of specific rates of net methyl mercury production in the water column and surface sediments of acidified and circumneutral lakes. Can. J. Fish. Aquat. Sci. 44, 750–757.
Yin, R., Feng, X., Wang, J., Bao, Z., Yu, B., Chen, J., 2013. Mercury isotope variations between bioavailable mercury fractions and total mercury in mercury contaminated soil in Wanshan Mercury Mine, SW China. Chem. Geol. 336, 80–86.
Zhang, T., Kim, B., Levard, C., Reinsch, B.C., Lowry, G.V., Deshusses, M.A., Hsu-Kim, H., 2012. Methylation of mercury by bacteria exposed to dissolved, nanoparticulate, and microparticulate mercuric sulfides. Environ. Sci. Technol. 46, 6950–6958.
Zhong, H., Wang, W., 2009. Controls of dissolved organic matter and chloride on mercury uptake by a marine diatom. Environ. Sci. Technol. 43, 8998–9003.